

## Sedimentation Processes and History Under the Northern Iberian Upwelling System

I.R. Hall<sup>1</sup>, I.N. McCave<sup>1</sup> & R. Bao<sup>2</sup>

<sup>1</sup>Department of Earth Sciences, University of Cambridge, Downing Street, Cambridge, CB2 3EQ, UK

<sup>2</sup>Área de Xeoloxía Universidade da Coruña, Campus da Zapateira s/n, 15071 A Coruña, Spain

### Introduction

The contribution of the University of Cambridge to OMEX II is as follows:

80% Work Package III Fluxes and Processes in the Nepheloid Layers and Surface Sediments

20% Work Package IV Integrated Margin-Exchange Product

1. will determine SPM concentration and composition (III.1.1)
2. will make particle accumulation and mixing rate determinations in boxcore sediments (III.1.3)
3. will measure sediment grainsize, diatom contents and <sup>13</sup>C isotope determination of organic carbon (III.1.4)
4. will make comparison with results OMEX I at Goban Spur (III.1.5)
5. will determine downcore variability of sediment composition and properties in long (Kasten) cores and will estimate eolian influence (III.1.7)
6. will make organic carbon determinations and C/N ratios for estimation of carbon burial fluxes
7. will estimate total SPM and POC as particulate components in the pelagic cycling of carbon (IV.2) and of particle fluxes and budgets
8. will analyse cores for the long-term record of benthic cycling and burial carbon (IV.5)
9. is responsible for estimating the sensitivity of upwelling systems to environmental change
10. will analyse cores for indicators of past upwelling cycles and distributions, and run model scenarios for varied climate forcing, to estimate sensitivity to climate change (IV.5)

This report provides an overview of the first years work carried out in the Department of Earth Sciences at Cambridge in support of the OMEX II objectives as outlined above.

### Suspended sediment distribution (items 1 & 4)

We have collected a total of 94 CTD stations providing detailed hydrographic data on temperature, salinity, oxygen, fluorescence, transmission and scattering obtained during two cruises: *RRS Charles Darwin* cruise number 105 (CD105; 29 May 1997-22 May 1997) and 110 (CD110; 23 Dec 1997- 19 Jan 1998) providing moderate temporal coverage.

During CD105 a grid of CTD stations, typically 10 km apart, on cross-slope sections at 43°N, 42°50', 42°40', 42°30', 42°20', 42°09', 42°N 41°48'N and 41° 25'N Sections N-V respectively) were occupied, while during CD110 inclement weather conditions limited the extent of CTD casts possible and coverage was rather poor (Fig 1).

All optical attenuation measurements were made with two 0.25-m-path-length SeaTech transmissometers. The transmissometer operates with light at 660 nm (red) wavelength to eliminate attenuation by dissolved organic substances (Jerlov, 1976). There is substantial literature relating to the SeaTech instrument and its performance in nepheloid layers (Bartz *et al.*, 1978; McCave, 1983; Gardner *et al.*, 1985; Bishop, 1986). Deployment protocols, including measurement of air values, followed the recommendations of McCave (1989; 1994). Light scattering was determined with a Sea-Tech Light Scattering Sensor (LSS) which measures infra-red light (880 nm) scattered from suspended particles in the sample volume using a solar-blind silicon detector. The full scale range of 5V is approximately 10mg/l. Deployment and calibration followed the manufacturers recommendations.

As the size, shape and refractive index of the suspended material in the water column vary from place to place a single literature equation cannot be used to relate attenuation to suspended matter concentration (McCave, 1983; Baker and Lavelle, 1984; Gardner *et al.*, 1985; Moody *et al.*, 1986; Gardner, 1989). It is therefore necessary to perform an empirical calibration of the transmissometer and LSS based on estimates of SPM concentration ( $\mu\text{g/l}$ ) in discrete water samples. Our calibration, based on 43 samples from 31 CTD stations taken in layers of high optical turbidity (INLs and BNLs) and clear water, is shown in Fig. 2.

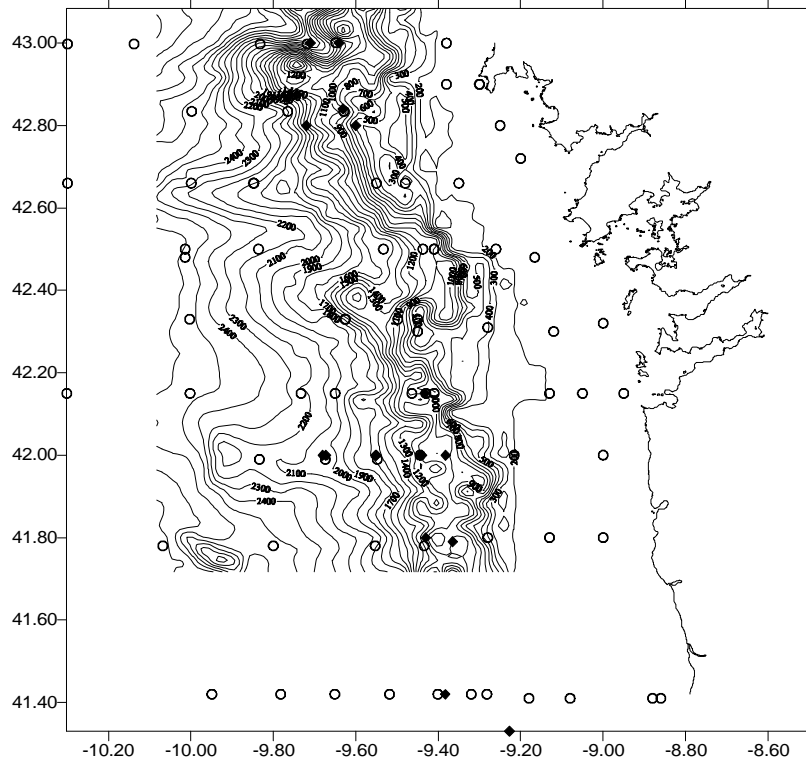


Fig. 1: Position of CTD casts during CD105 (open circles) and CD110 (filled diamonds) together with Seabeam bathymetry collected during CD105 (see report of Huthnance).

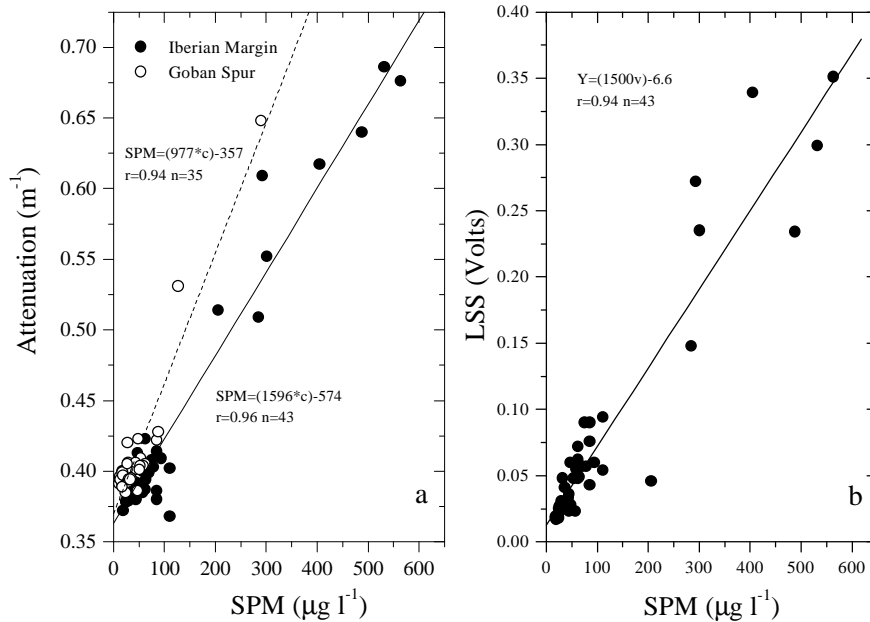
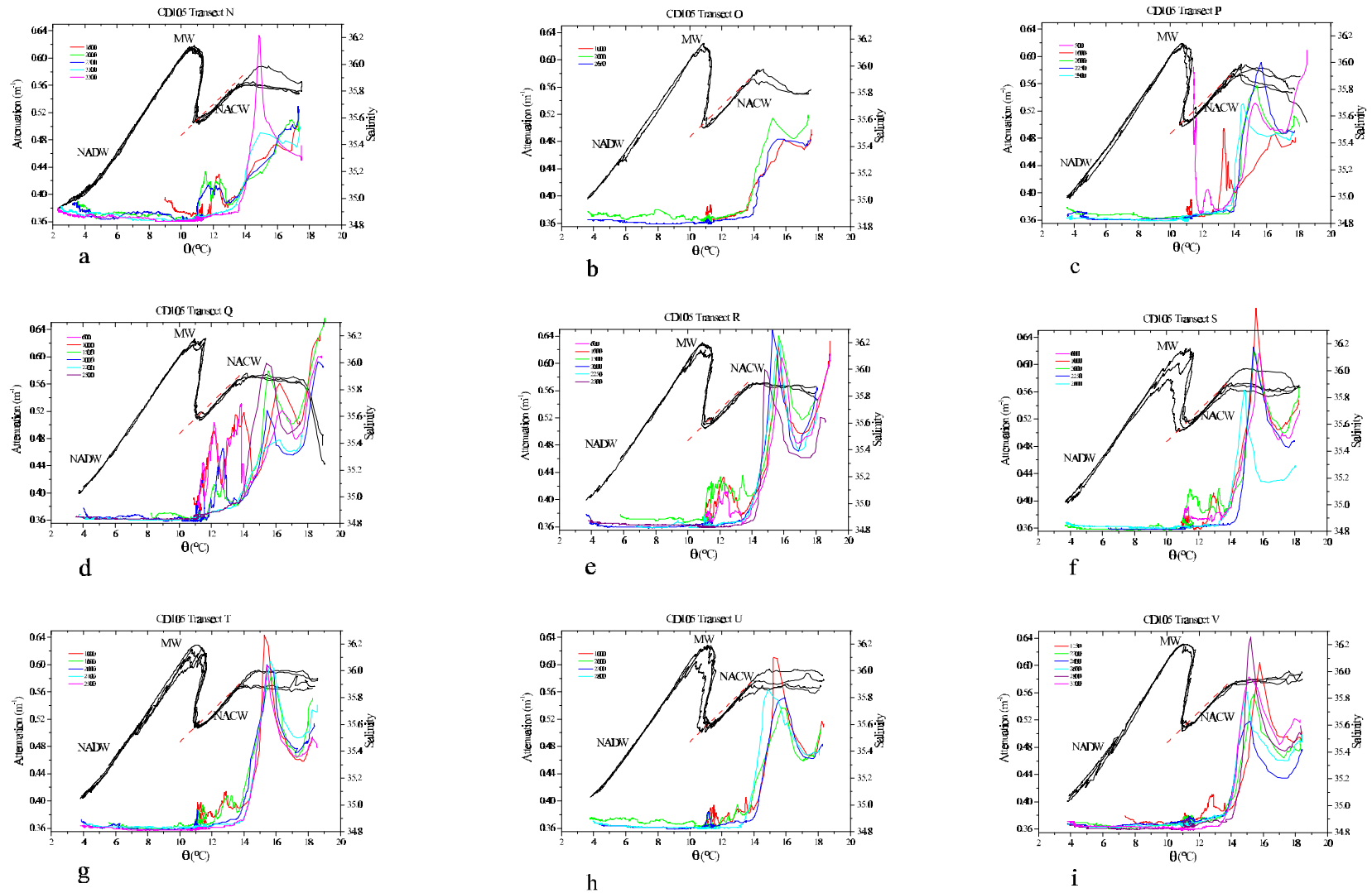


Fig. 2: Transmissometer (a) and LSS (b) calibration. Goban Spur (dashed) calibration shown for comparison

Fig 3. (a-i) Potential temperature versus salinity (upper curves) and potential temperature versus attenuation (lower curves) for stations greater than 500 m during CD110. Note the major spike in attenuation at  $\sim 15^\circ\text{C}$  is the SNL associated with the thermocline, the presence of INL's in the NACW but very little in MW, and weak BNL's in NADW.



Pure (particle free) sea water has a percent transmission of 660 nm light (red) per 0.25 m of 91.3%, corresponding to an attenuation coefficient of  $c_w=0.364$  according to SeaTech (Sea Tech Inc.), and  $c_w$  is 0.358 according to Bishop's (1986) empirical determination for seawater *in situ*. These figures are close to the  $c_w$  of 0.361 suggested by our calibration. Calibration of the LSS was also satisfactory, with extrapolation of the calibration to full scale giving a value close to the manufactures nominal operational range

It should be stressed that satellite images and CTD profiles indicate that upwelling was not present during the duration of CD105 and therefore the SPM distribution therefore represent a pre-upwelling summer conditions. SPM distribution for each off-slope section during CD105, based on attenuation, together water mass structure is shown in Fig.3. (a-i) (for station deeper than 500 m). Profiles typically show a subsurface peak in particle load associated with the thermocline. Intense intermediate nepheloid layers are seen in in North Atlantic Central Water (NACW), underlain by relatively turbidity free Mediterranean Water (see below). North Atlantic Deep Water (NADW) is mostly represented by low particle concentrations typical of clear water ( $\sim 8-15 \mu\text{g l}^{-1}$ ), although some higher turbidity INL's are observed. There appears to be only limited bottom nepheloid activity particularly at depth suggesting weak off-shelf transport of material and weak current resuspension.

Profiles from CD110 are not shown but generally agree in structure and extent to those seen in CD105.

The spatial data coverage achieved during CD105 has allowed us to explore visualisation techniques and the data have been contoured using the plotting program of Rudniki (1997). An example section for attenuation is shown in Fig.4. The bathymetry in these sections is the linear track between CTD stations from the Seabeam bathymetry. In order to visualise the data, but not get in to the 'aquafantasy' problems of 3D volumetric plotting, fence diagrams have been constructed which retain a fidelity to the essential two-dimensional nature of the underlying data. These diagrams suggest the important role of canyons and chutes in the export of particulate material to the deep ocean. In particular they highlight the presence of a high turbidity plume of near surface low salinity water ( $\sim 15-20$  m depth) along section 'Q' (see below and Fig 3. D)

#### Mediterranean Outflow Water

Figure 5 and 6 show the maximum salinity associated with MW during CD105. The salinity core of 36.150 agrees with values previously reported for this region (Daniault *et al* 1994). The turbidity associated with MW showing off-slope decrease to clear water is perhaps surprising suggesting that MW only picks up a small amount sediment where it impinges directly on the slope, and that this does not spread laterally across the water mass.

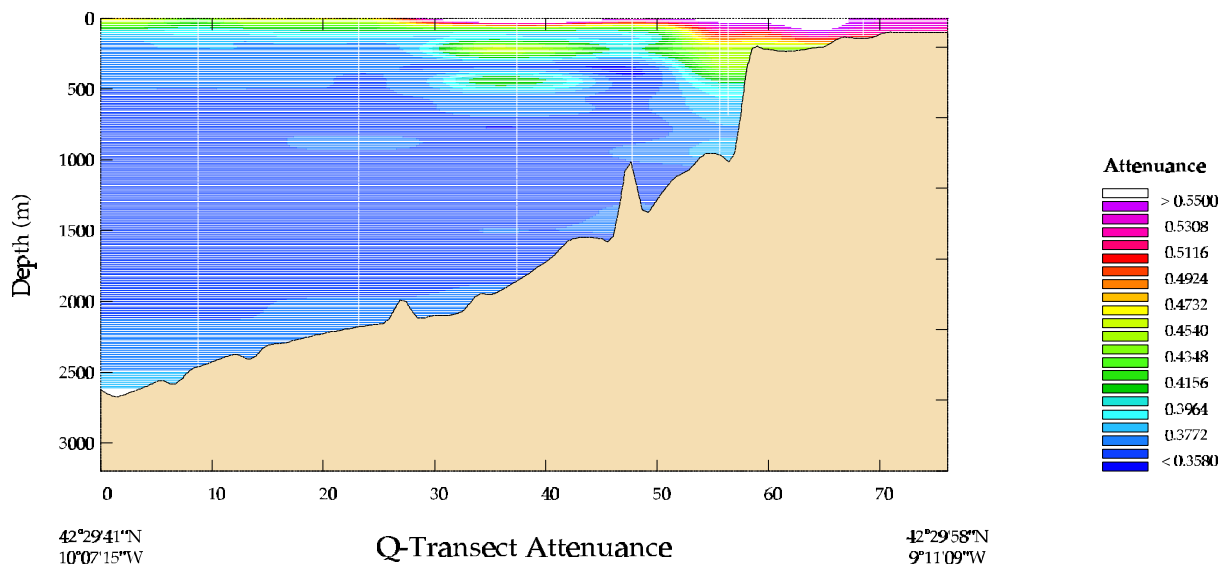


Fig. 4: Contour sections of attenuation (top) and sigma-t (bottom) used to generate fence diagrams.

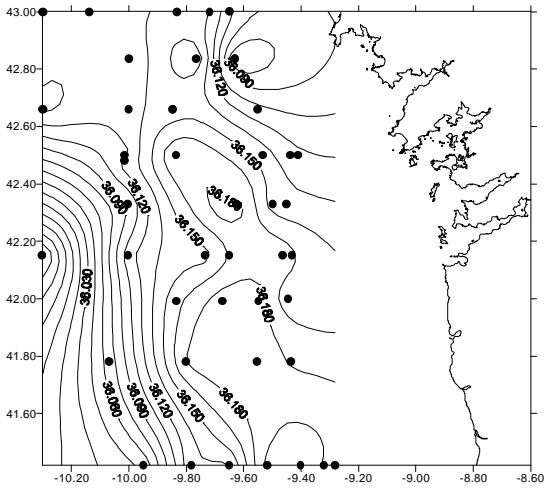


Fig. 5: Salinity maximum in MW

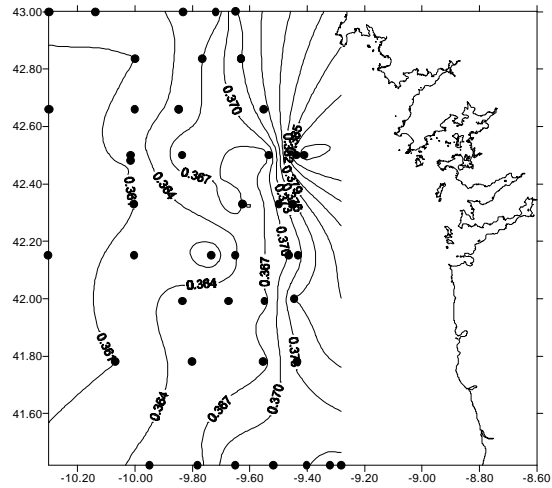


Fig. 6: Attenuation at salinity maximum of MW

*Comparison of Light Scattering and Attenuation.*

Calibration of instruments to spm load allows a direct comparison between the measurement of attenuation and scattering.

Figures 7 and 8 show comparisons between all casts to greater than 500m depth and highlight the differences in the relationship in the SNL. Figure 9 shows a typical comparison of attenuation and scattering profiles with depth.

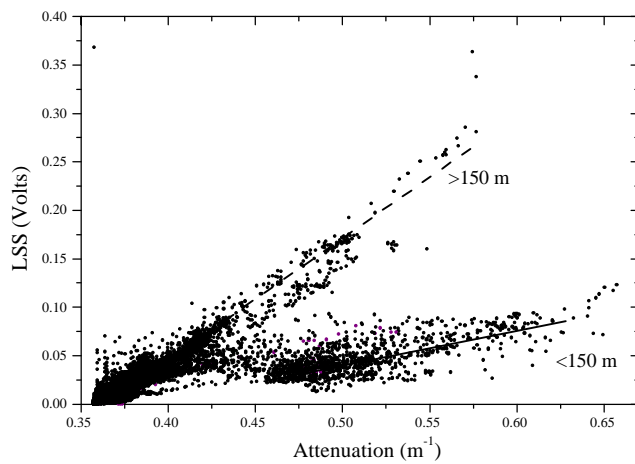


Fig. 7: Comparison between transmissometer and LSS for all stations >500 m water depth during CD105 (Summer pre-upwelling conditions).

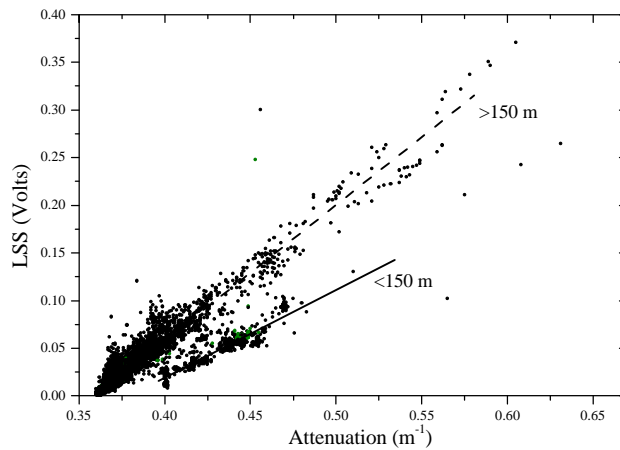


Fig. 8: Comparison between transmissometer and LSS for all stations >500 m water depth during CD110 (Winter). Note the closer agreement between the instruments in the surface nepheloid layer.

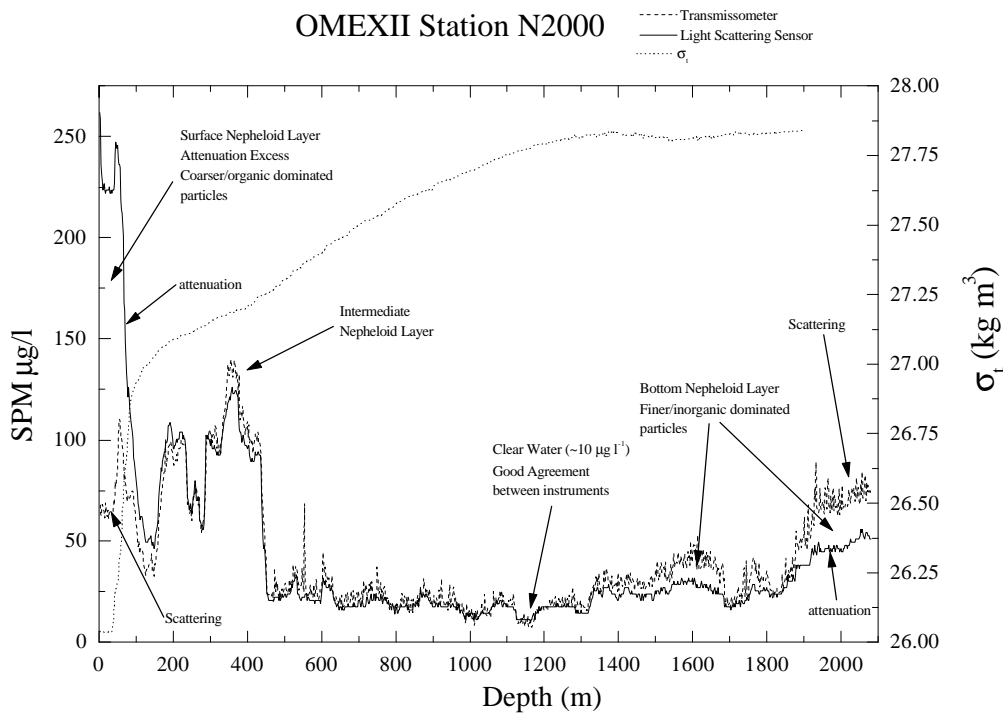


Fig. 9: Showing typical profile of attenuation and scattering particle loads against depth, together with sigma-t water structure.

Differences between the signals may provide information on the particle population. Figure 10 shows the integrated attenuation excess (over scattering load) particle load for the upper 150 m in water depths greater than 500 m, below this depth the clear water minimum cannot be used to check instrumental consistency. Further work is needed to establish if this excess is directly related to the organic carbon load but, if a rather conservative conversion of 0.4 is used, these reasonable values of the organic carbon load in the SNL are indeed obtained. These data show also a weak positive relationship with the mean temperature ( $R=0.45$ ) over 150 m and may be indicative of pre-upwelling conditions as the opposite would be expected during upwelling events.

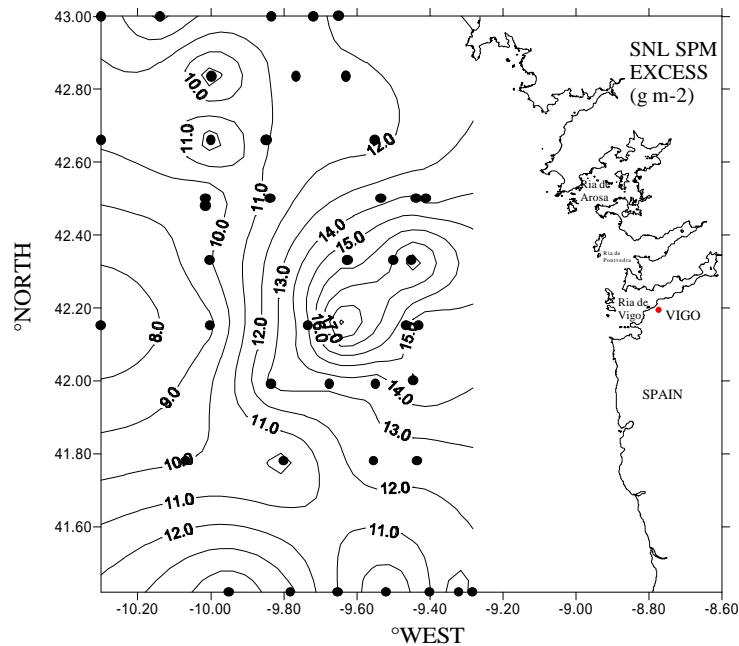


Fig. 10: Attenuation excess integrated over the upper 150 m

### Sediments

Sediments are often the ultimate repository of many elements in the oceanic system. Studies over a year or two at present simply provide a snapshot of a variable system. The long-term output sink for sediment, organic and inorganic carbon is the sea-bed of the margin and the nearby offshore. Accumulation varies in relation to changing climate, of which the most dramatic example was the last deglaciation, ending some 11,000 years ago. Within the last 10,000 years there have also been significant climate shifts of lesser magnitude, of which the most recent was the Little Ice Age from about 1400 to 1890 AD. Understanding of the system as a whole needs the historical perspective provided by analysis from cores covering the deglaciation and Holocene through to the present.

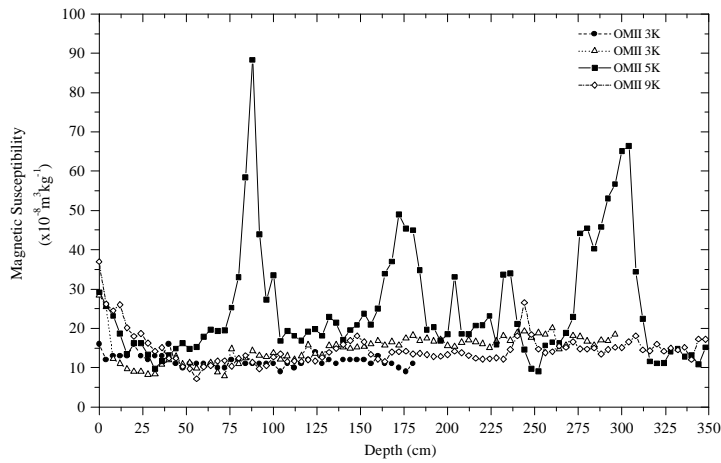
We have collected a total of 4 kasten (Table 1) and 7 box cores from the OMEX II Region.

CRUISE	CORE OMI-	DATE	TYPE	CORE LENGTH (cm)	LATITUDE (N)	LONGITUDE (W)	WATER DEPTH (m)
CD 105	2K	31/5/97	4 m KASTEN	180	41° 47.43'	09° 26.90'	1152
CD 105	3K	1/6/97	4 m KASTEN	300	41° 47.22'	09° 29.75'	1610
CD 105	5K	3/6/97	4 m KASTEN	353	41° 49.52'	10° 01.04'	2723
CD 105	9K	7/6/95	4 m KASTEN	350	42° 19.94'	09° 41.91'	1833

Table 1., Kasten core sampling data.

Measurements of bulk magnetic susceptibility (BMS) were made every 2 cm downcore using a Bartington Instrument MS2 meter with a 'probe'-type sensor held against sediment slabs. Magnetic susceptibility of the coarse and fine fraction was also measured on dried samples using a Bartington BS2B sensor with a 36-mm internal diameter cup. Weight corrected BMS for each of the kasten cores is shown in Figure 11.

Variation in magnetic susceptibility in deep sea sediments reflects changes in lithology, such as the ratio of biogenic to lithogenic components, and therefore provides a rough guide to concentrations of



terrigenous material (Robinson and McCave, 1994). The most prominent features of BMS and WC profiles in the continental margin setting of the OMEXII study area are turbidites and pulses of ice-rafted debris (Heinrich events) which both deliver a large quantity of lithic material of diverse mineralogy to the sea bed in a short time.

Fig. 11: Weight corrected bulk magnetic susceptibility for OMI 3 kasten cores.

Total carbonate and organic carbon content of the OMEXII kasten cores is shown in Figure 12 and 13 respectively.

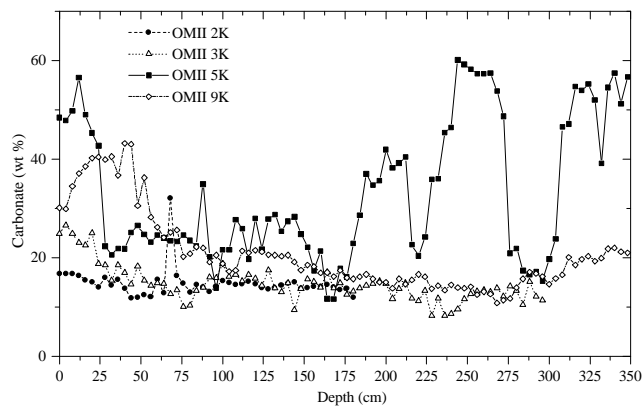


Fig. 12: Total carbonate content of OMEX II kasten cores

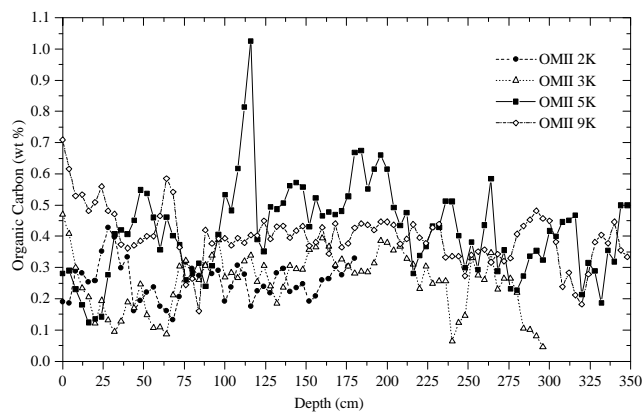


Fig. 13: Total organic carbon content of OMEX II kasten cores

Particle size analysis of the non-carbonate fraction <63  $\mu\text{m}$  has been completed for cores OMII 5K and 9K and will be used to evaluate the fluctuation in bottom current strength over the time period of the cores. For the sandy core OMII 3K grain-size of the sand fraction is shown in Figure 14.

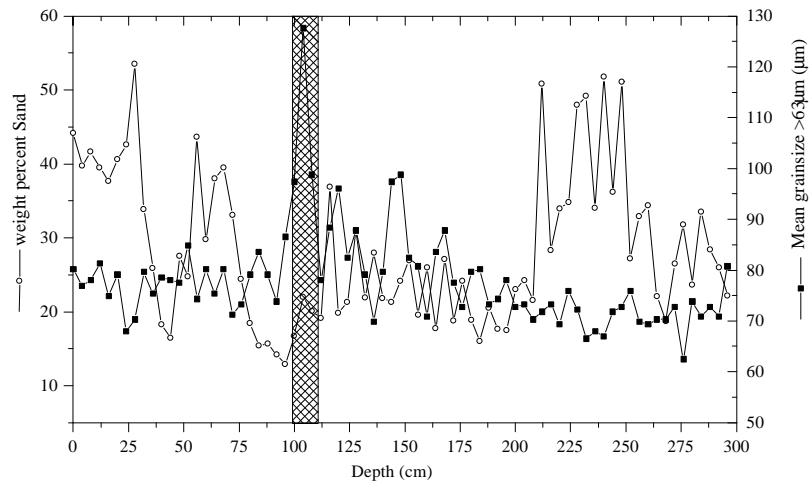


Fig. 14: Amount and mean grainsize of the sand component in core OMII 3K. Hatched area shows the presence of a layer of pteropod fragments.

#### Diatom analysis

Work carried out by Universidade da Coruña aims to a) establish by means of diatom analysis in bottom sediments the relationship between present day oceanographic conditions and the contemporary sedimentary record in across slope transects of the NW Iberian and b) to help in the reconstruction of the paleoceanography of the region, back to the last glacial maximum, using downcore diatom assemblages mainly as indicators of upwelling, paleoproductivity and freshwater influence.

Diatom content in both transects was very poor mainly consisting in valve fragments. Scarcity of diatoms in the slides did not allow confident quantitative estimates of absolute or percent diatom abundances. Qualitative analysis showed however that inshore stations had a lower diatom content than offshore ones. Samples of stations OMII-7B, 8B and OMII-1B, 2B and 2K were almost barren. Offshore stations showed a higher diatom content with a peak at station OMII-5B. Although only qualitative, this result agrees with the known offshore diatom increase from the shelf break occurring in the northern Portuguese coast (Abrantes, 1988).

Whole diatom valves consisted in robust taxa as *Paralia sulcata*, *Azpeitia nodulifer*, *Chaetoceros* resting spores or copulae of *Thalassiosira*. More delicate forms as *Thalassiosira* spp. valves also occurred in some cases but diatom diversity in the samples was always poor. Surprisingly, *Chaetoceros* resting spores did not attain an outstanding relative presence (with the exception of OMII-5B) in spite of its upwelling related affinity and high resistance to dissolution. Benthic and tychopelagic diatom taxa whose life is restricted to neritic environments (*Actinoptychus senarius*, *Paralia sulcata*, *Rhaphoneis* spp. or *Diploneis* spp.) were recorded even in the most offshore stations indicating the effects of lateral transport.

Almost all the samples contained sponge spicules and silicoflagellates, with a minor presence of phytoliths. Whole radiolarian skeletons and ebridians were restricted to the most offshore samples (specially OMII-5B and 5K).

Although mass sediment accumulation rates are still lacking, obtained qualitative results might indicate a strong contrast with diatom content at the Goban Spur Margin where diatom accumulation rates could reach as high as  $180 \times 10^6$  valves  $\text{cm}^{-2} \text{Ka}^{-1}$  due to the effect of strong downslope advective fluxes at the deeper positions.

### References

- Bartz, R., Zaneveld, J.R.V. & Pak, H.** (1978) A transmissometer for profiling and moored observations in water. *Proc. Soc. Phot-opt Instrum. Engrs.*, **160**, 102-108.
- Baker, E.T and Lavelle, J.W.** (1984) The effects of particle size on the light attenuation coefficient of natural suspensions. *Journal of Geophysical Research*, **89**, 8197-8203.
- Bishop, J.K.B. and Joyce, T.M.**(1986) Spatial distributions and variability of suspended particulate matter in warm core ring 82B. *Deep Sea Research*, **33**, 1741-1760.
- Daniault, N. Maze, J.P and Arhan, M.** (1994) Circulation and mixing of Mediterranean Water of the Iberian Peninsula. *Deep Sea Research*, **41**, 1685-1714.
- Gardner, W.D.** (1989) Baltimore Canyon as a modern conduit of sediment to the deep sea. *Deep-sea Research*, **36**, 323-358.
- Gardner, W.D., Biscaye, P.E., Zanveld, J.R.V. and Richardson, M.J.** (1985) Calibration and Composition of the LDGO nephelometer and the OSU transmissometer on the Nova Scotian Rise. *Marine Geology*, **66**, 323-344.
- Jerlov, N.G.** (1976) *Marine Optics*. Elsevier, New York, 231pp.
- McCave, I.N.** (1983) Particulate size spectra, behaviour and origin of nepheloid layers of the Nova Scotian Continental Rise. *Journal of Geophysical Research*, **88**, 7647-7666.
- McCave, I.N.** (1984) Erosion, transport and deposition of fine-grained marine sediments. In: Fine-Grained Sediments: Deep Water Processes and Facies. Geological Society of London Special Publication, **15**, 35-69.
- McCave, I.N.** (1989) Leg 3, Benthic studies, of the Biogeochemical Ocean Flux Study between 47°N and 60°W in the northeast Atlantic Ocean. Cruise Report, RRS Discovery 184, University of Cambridge, Dept. of Earth Sciences, 4xpp.
- Moody, J.A. Butman, B. and Bothner, M.H.** (1986) Near-bottom suspended matter concentrations during storms. *Continental Shelf Research*, **7**, 609-628.
- Rudniki, M. D.** (1997) A computer program for plotting oceanographic fence diagrams. *Computers and Geosciences*, **23**, 209-213.